Wind Tunnel Investigation of the Transonic Aerodynamic Characteristics of Forward Swept Wings

G.C. Uhuad,* T.M. Weeks,† and R. Large‡
Air Force Wright Aeronautical Laboratories, Wright-Patterson Air Force Base, Ohio

This paper discusses some of the results of a series of wind tunnel investigations conducted on forward and aft swept wings in order to compare the relative drag performance of both wings at a transonic maneuver condition and to determine the associated drag penalty of the forward swept wing for a high supersonic cruise condition. At the transonic maneuver design point, the results indicate a significant reduction in the profile drag of the forward swept wing relative to the aft swept wing. The forward swept wing exhibits extreme sensitivity to wing root height and incidence variations. A drag penalty was recorded at $M=2.0$ for the forward swept cruise wing. The cruise wings have the same sweep and "box" geometries as the transonic maneuver wings. The difference in supersonic cruise drag is attributed to the difference in the leading-edge sweeps ($\Lambda_{LE} = +48.7$ and -28 deg for the aft and forward swept wings, respectively). This drag penalty decreases at lower supersonic Mach numbers. The results of the test indicate that the aft swept wing aerodynamic design and analysis methods used in the study can be used on forward swept wings with only minor modifications.

Nomenclature

$\mathcal{R}$	= aspect ratio
ASW	= aft swept wing
b	= span, ft
BL	= butt line, ft
c	= section chord, ft
C_{avg}	= average geometrical wing chord
C_D	= drag coefficient = D/qs
$(C_{D_L})_{prof}$	= profile drag coefficient due to lift
C_{D_i}	= induced drag coefficient
$C_{D_{min}}$	= minimum drag coefficient
C_L	= lift coefficient = L/qs
C_l	= section lift coefficient
$\mathfrak{L}$	= fuselage centerline
C_P	= pressure coefficient = $(p-p_\infty)/q$
c.p.	= center of pressure
e	= span efficiency factor
FSW	= forward swept wing
L/D	= lift-to-drag ratio
M	= Mach number
MAC, $\bar{c}$	= mean aerodynamic chord
q	= dynamic pressure
Re	= Reynolds number
Sw	= wing reference area, ft^2
Sc	= canard reference area, ft^2
t/c	= thickness ratio
x/c	= percent chord
$y/b, \eta$	= spanwise station
α	= angle of attack, deg
β	= sideslip angle, deg
Λ_{LE}	= leading-edge sweep angle, deg
Λ_S	= shock sweep, deg
τ	= taper ratio

Received June 29, 1981; revision received April 12, 1982. This paper is declared a work of the U.S. Government and therefore is in the public domain.

*Aeronautical Engineer.
†Technical Manager, External Aerodynamics Group. Associate Fellow AIAA.
‡Aerospace Engineer.

Introduction

An investigation of a forward swept wing (FSW) vs a state-of-the-art aft swept wing (ASW) was conducted to compare the relative performance of both wings at a transonic maneuver condition ($C_L=0.9$, $M=0.9$) and to determine the associated drag penalty of the FSW for a high supersonic cruise condition ($C_L=0.075$, $M=2.0$). The results indicate a significant reduction in transonic profile drag for the FSW relative to its ASW counterpart. A drag penalty was recorded for the forward swept cruise wing at $M=2.0$. This latter wing was designed to represent the same sweep and "box" geometry as the transonic maneuver wings. This investigation was conducted under a joint effort by the USAF AFWAL/Flight Dynamics Laboratory and Grumman and is reported in Ref. 1.

Discussion

The concept of forward swept wings is not entirely new. In the investigation of the methods of delaying the onset of drag rise for flight in the vicinity of the speed of sound, it was found that wing sweeping provides a very effective means of increasing the drag divergence Mach number. Aerodynamically, the same effect can be obtained regardless of the direction of sweep. However, previous swept wing designs have favored the use of aft sweeping in order to avoid the phenomenon of wing structural divergence inherent on forward swept wings operating under a high dynamic pressure condition, which cannot be solved through conventional metallic structures without paying an excessive wing weight penalty. Structural divergence is that phenomenon in which the FSW wing outboard panels deflect under air loads, such that the direction of deflection results in an increase in panel angle of attack. This, in turn, causes further increases in air load and so on. This aeroelastic effect is due to the relative location of the panel center of pressure and the wing elastic axis. Highly swept forward wings of conventional structure generally have elastic axes running aft of the panel center of pressure. This arrangement causes deflections under load resulting in increases in panel alpha. The coupling effect continues and the result may be disastrous if the wing structural divergence Mach number is exceeded. This problem does not exist on conventional aft swept wings. In fact, the location of the axis ahead of the center of pressure prevents the occurrence of this condition. Recent advances in com-

posite materials technology are now providing a promise of eliminating the divergence problem on FSW with little or no wing weight penalty. With composite materials, the wing skin laminates can be tailored to provide favorable wing deflections at Mach numbers considerably higher than those previously attained with conventional structures.[2]

Until the advent of composite materials, very few forward swept wing aircraft were designed, and only a limited number were actually built and flown. Some notable examples (Fig. 1) include the Junkers JU-287, which flew over a dozen times before being damaged by allied bombers in World War II; the HANSA HFB 320, which is currently operational as a business jet; and the FANTRAINER RBI-ATI-2, a newly developed slightly swept forward trainer. Other design examples (Fig. 2) include the CONVAIR XB-53, Heinkel He 162, and the BLOM and VOSS P290.02. Recently renewed interest in forward swept wing investigations, stimulated by the advances in composite materials, has provided several new designs.

Several potential benefits of forward swept wings have been identified. From a configuration standpoint, it provides reduced takeoff gross weight, volume benefits, and expanded design configuration flexibility. From purely aerodynamic considerations, forward swept wings may provide extended high angle of attack lateral controllability, higher spin resistance, improved low-speed handling qualities, lower stall speeds, and reduced transonic maneuver drag. A forward swept wing flow separation pattern generally starts from the root and gradually propagates outboard, allowing attached flow to be maintained over the outboard wing panels, thereby retaining aileron effectiveness at high angles of attack where aft swept wings may exhibit lateral control degradations.

The origin of the theoretical transonic drag advantage may be considered in two ways. The first consideration is that in comparing forward and aft swept wings in transonic flow, if the leading-edge sweeps, shock locations, taper ratios, aspect ratios, and wing areas are made identical, the resulting shock sweep of the forward swept wing is higher as shown in Fig. 3. This higher shock sweep of course equates to a lesser wave drag for the FSW. A second consideration is that if both wings are designed under equal aerodynamic conditions (lift coefficient and Mach number), keeping aspect ratios, taper ratios, shock sweeps, and shock locations equal (Fig. 4), the resulting leading-edge sweep of the FSW is less than the ASW. If flow remains attached at the leading edges of both wings, the drag of the FSW will be smaller owing to a higher streamwise component of the leading-edge suction. In addition, experimental investigations have shown that certain supercritical wing designs exhibit a reduction in profile drag with decreasing leading-edge sweep. Further discussions on this finding follow.

Drag of a wing consists of the minimum drag and the drag associated with the production of lift (Fig. 5). Drag due to lift consists of the contributions of the profile drag due to lift and the induced drag. The former results from an increase in profile drag from its minimum value when the separation point moves forward and the wake thickens owing to the generation of lift on the airfoil and shock wave drag. The latter is caused by the formation of the downwash in the presence of wing trailing vortices. The theoretical transonic drag advantage of the FSW over an ASW investigated under

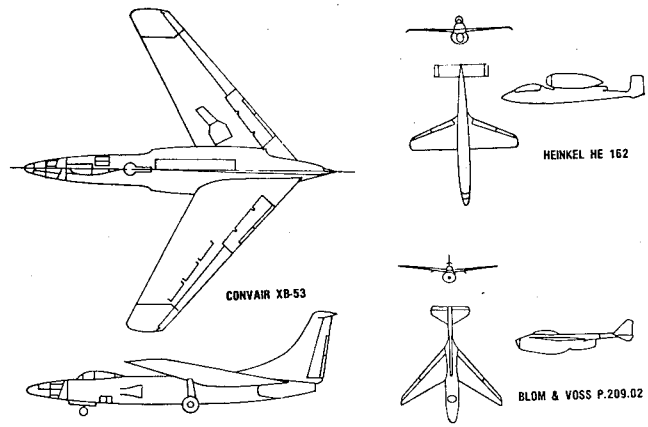

Fig. 2 Forward swept wing designs.

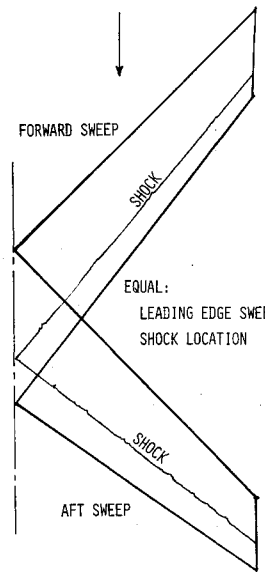

Fig. 3 Equal leading-edge sweeps.

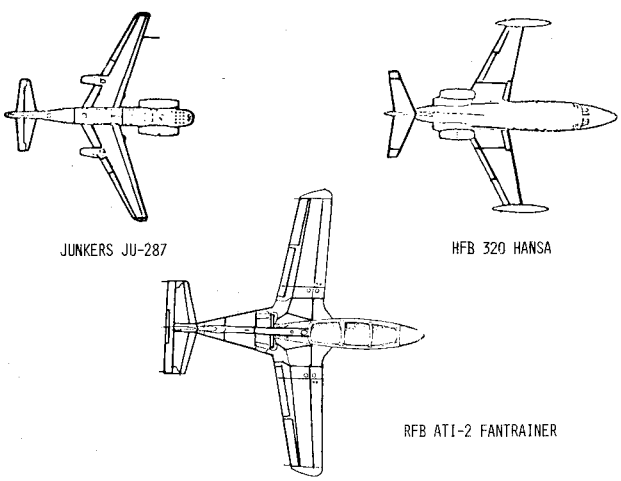

Fig. 1 Forward swept wing aircraft.

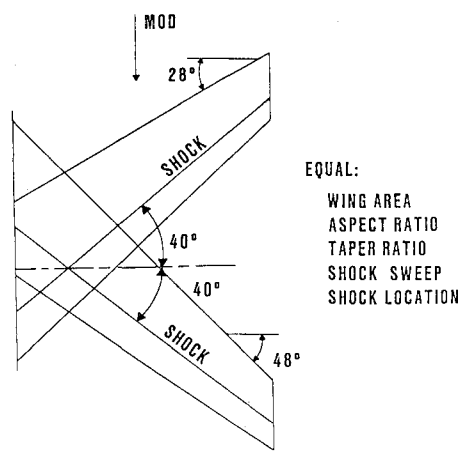

Fig. 4 Equal shock sweeps.

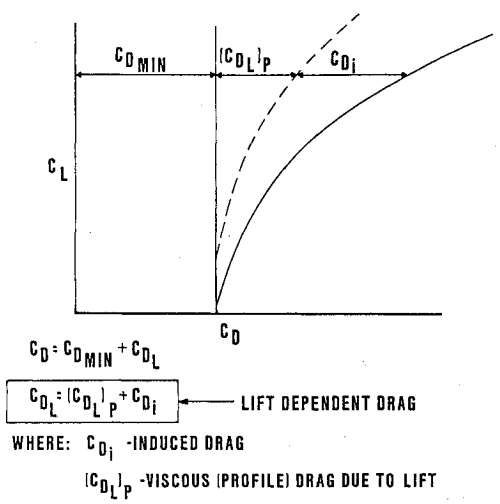

Fig. 5 Drag breakdown.

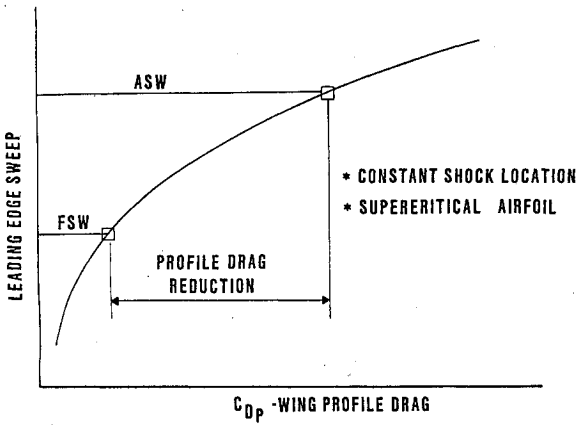

Fig. 6 Profile drag.

the current study are due to the two lift dependent components of drag which can be shown to be less on a FSW when both wings are designed under identical transonic design conditions.

Profile Drag Due to Lift

Experimental investigations conducted by Grumman on a series of supercritical wings under the HiMAT studies have shown a direct relation between leading-edge sweep and profile drag at transonic maneuver lift conditions. Analysis of the data showed that while maintaining shock location and utilizing the Grumman supercritical "K" airfoil, the profile drag decreases with decreasing leading-edge sweep at a maneuver lift coefficient ($\simeq 0.92$) in a manner shown in Fig. 6. In applying the conditions of identical shock sweeps, shock locations, aspect ratios, and taper ratios on forward and aft swept wings, the resulting leading-edge sweep of a forward swept wing is less than that of the aft swept wing (Fig. 4). Hence, from Fig. 6, utilizing the same wing design method and the supercritical "K" airfoil, the FSW indicates a reduction in profile drag by a value proportional to the difference in the leading-edge sweep of both wings.

Induced Drag

The induced drag advantage can be explained as follows: Under a condition of equal lift and identical spanloads, the center of pressure of the FSW is more inboard along the swept span than the ASW (Fig. 7). Consequently, the bending moment about a pivot point can be considerably less. If the span of the FSW is then allowed to increase, while maintaining wing area, until the pivot bending moments are equal, the accompanying increase in aspect ratio decreases the induced drag. Figure 8 summarizes the origins of the FSW drag decrement investigated in this study.

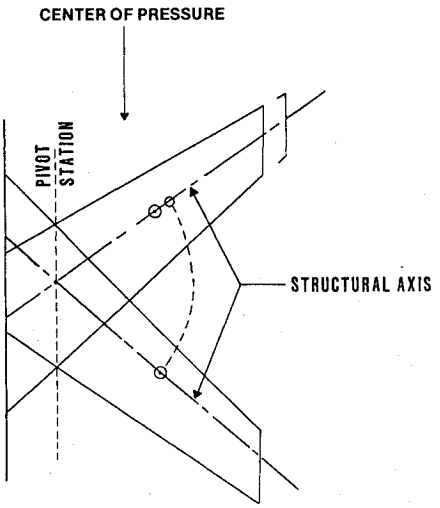

Fig. 7 Center of pressure comparison.

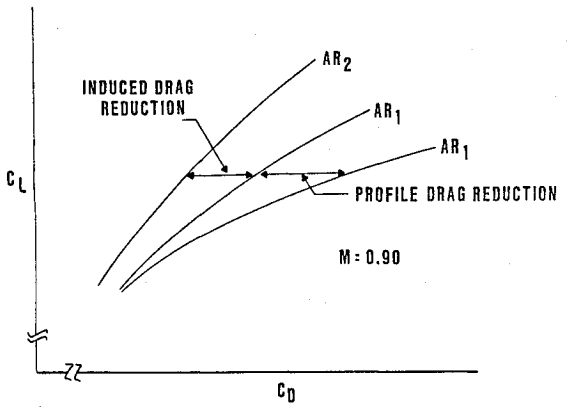

Fig. 8 Forward swept wing drag advantage.

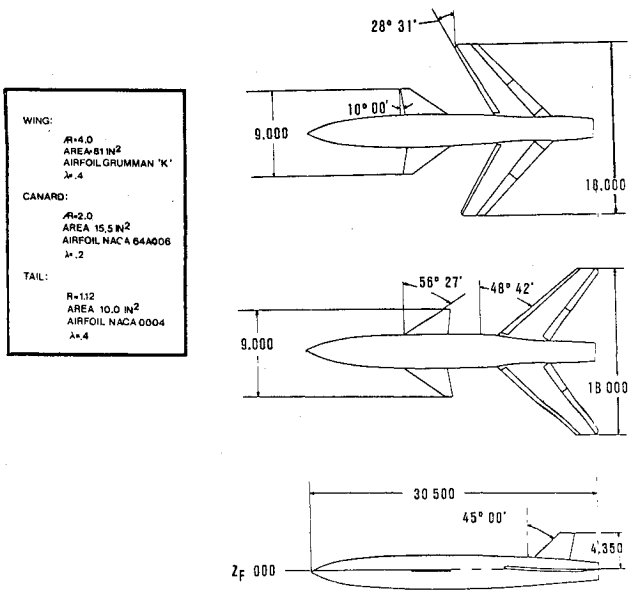

Fig. 9 Model general arrangement.

Model and Test Description

Tests were conducted in the 4 ft transonic tunnel of the Propulsion Wind Tunnel Facility of the Arnold Engineering and Development Center in 1978 and 1979. Details of the operating capabilities of this tunnel are discussed in Ref. 3. Tests were conducted over a Mach range from 0.6 to 1.3 and 2.0. The Reynolds number was fixed at (3.5×10^6)/ft. Six component force and moment data were taken along with model pressure data during the first and second entry. No pressure data were obtained during the third entry. Oil flow data were also obtained for all flow conditions.

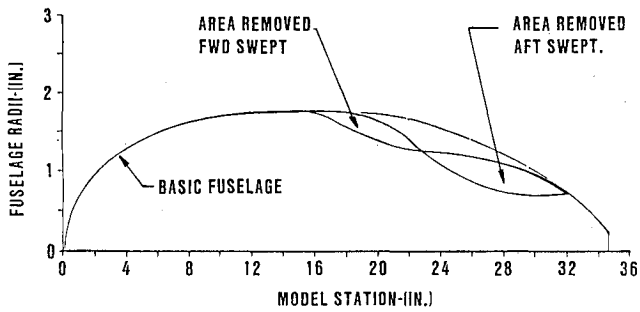

Fig. 10 Model area ruling.

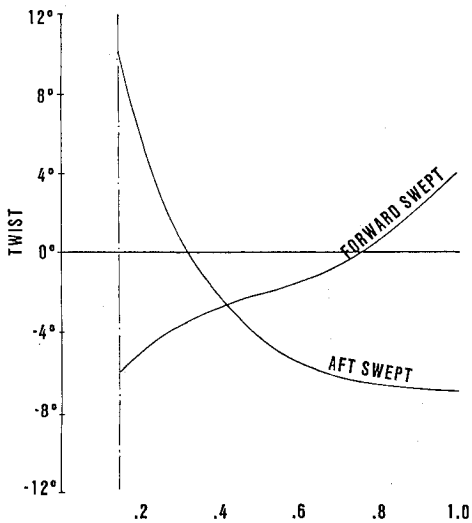

Fig. 11 Maneuver wing twist (first entry).

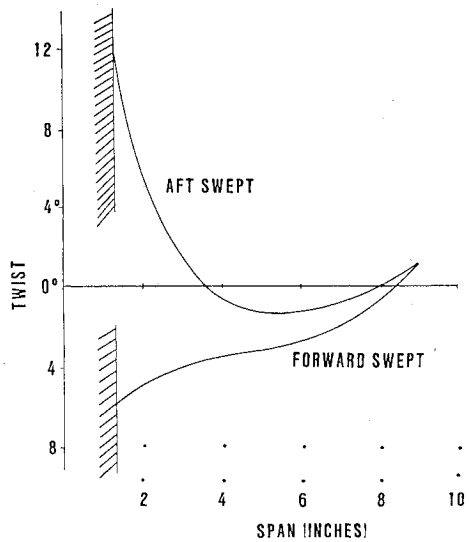

Fig. 12 Cruise wing twist (second entry).

Aerodynamically the same design ground rules and techniques were used for both forward and aft swept wings. Design aspect ratios, taper ratios, wing areas, shock locations, shock sweeps, airfoils, and spanloads were identical. Figure 9 shows the general arrangement of the forward and aft swept configurations. The supercritical wing design method, previously untested for forward swept wing configurations, was applied without modifications to provide the lines for the forward swept wings. The model was area ruled separately for the forward and aft swept wings (Fig. 10).

First Entry

This entry tested both forward and aft swept maneuver condition wings ($C_L = 0.9$, $M = 0.9$). The FSW required twist distribution is opposite but also reduced relative to the corresponding ASW (Fig. 11). The design shock sweep angles were ± 40 deg for the aft and forward swept wings, respectively. In this case, the ASW had a 48.7-deg leading-edge sweep, whereas the FSW had -28.7 deg. The FSW twist for this design was about 10 deg with a -5.8-deg wing root incidence. The ASW twist was 18 deg with an 11-deg wing root incidence. Both wings were designed to satisfy a high body condition. In transitioning the paper design to the practical model, wing fabrication difficulties made it virtually impossible to satisfy this high body design condition simultaneously. Part of the wing design process utilized a vortex lattice program to calculate the slopes of the wing elements required to support the design loads. This process provided twist and camber that were accurate for only one wing plane. After the calculated elemental surfaces were joined to provide a smooth continuous surface and, after the addition of the thickness envelope, the final wing contours varied considerably from the initial constant wing plane condition. For the FSW, satisfying the requirement for a high root leading-edge location was not possible without causing the root section crest point to exceed the maximum fuselage diameter. On the ASW, a high root leading edge placed the trailing edge close to the fuselage centerline. Therefore, for a compromise, the wing location criteria used was to make the heights of the quarter-chord points of the mean geometric chords identical.

Second Entry

This entry tested both FSW and ASW in their supersonic cruise configuration. Wing planform and height were derived from the first entry. Twist and camber were reduced on both wings. The aft swept wing total twist was 12 deg with a root incidence of 11 deg. The FSW total twist was 6.8 deg with a

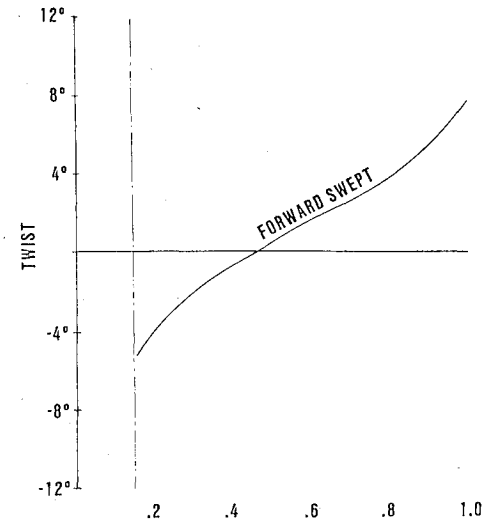

Fig. 13 Maneuver wing twist.

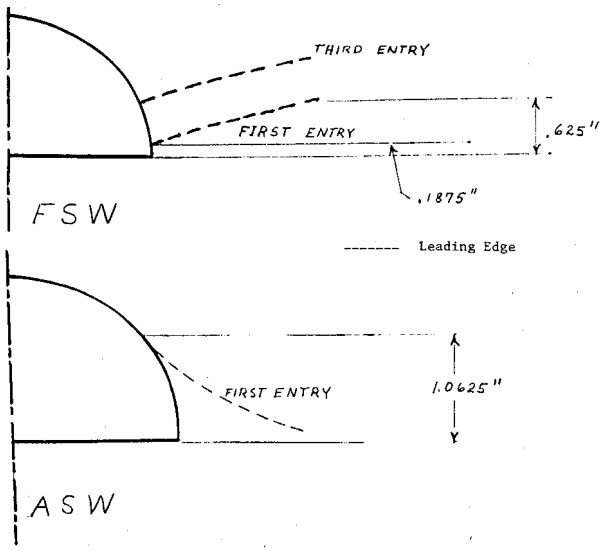

Fig. 14 Wing root leading-edge height comparison.

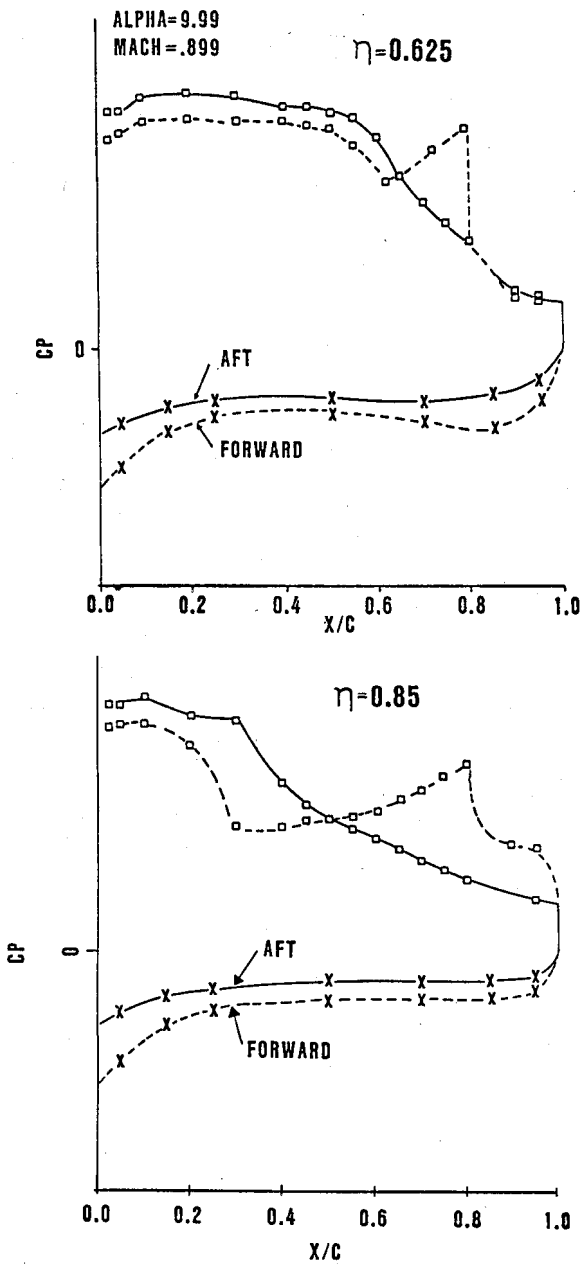

Fig. 15 Pressure distribution comparison (first entry).

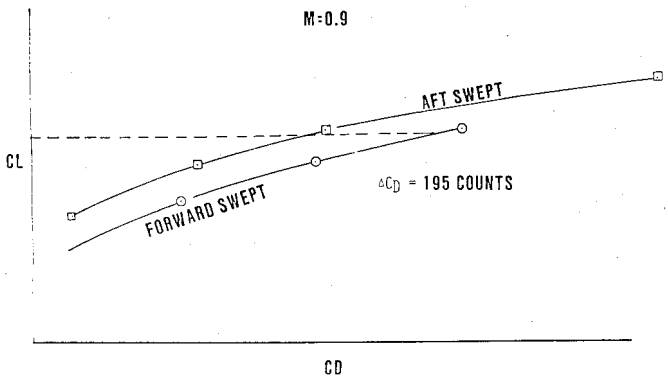

Fig. 16 Maneuver wing drag comparison (first entry).

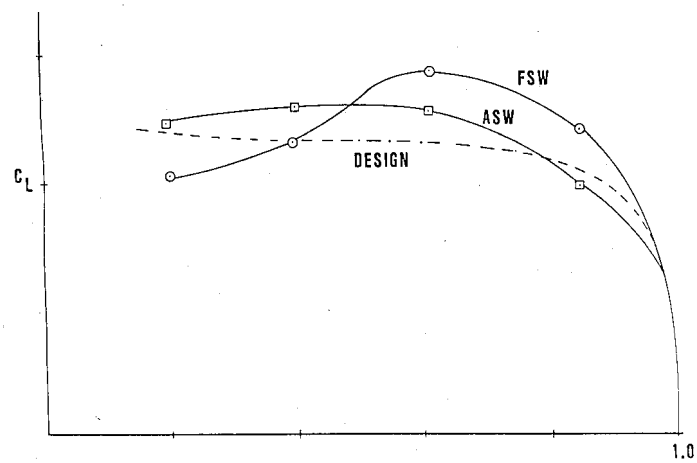

Fig. 17 Maneuver wing spanwise load comparison (first entry).

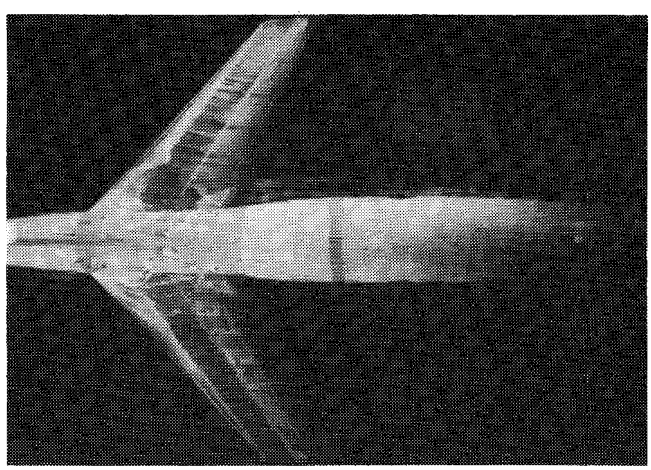

Fig. 18 Oil flows.

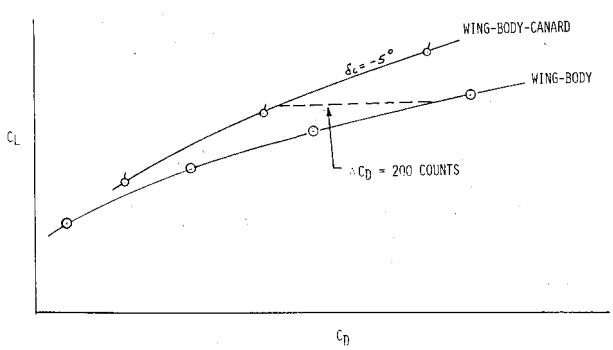

Fig. 19 Oil flows.

−5.8-deg root incidence (Fig. 12). The "box" geometry from 15% to 60% chord was made identical to the first entry wings. These configurations were not optimized for supersonic cruise. These wings were merely the decambered versions of the wings from the first entry. The amount of decambering was limited by the constraints imposed on the wing box.

Third Entry

The initial wing location criteria used during the first entry had resulted in the FSW being mislocated such that the wing root was operating in a region of excessive fuselage upwash. The final entry tested only the modified FSW maneuver case. Wing height was changed so that the crest point of the centerline airfoil coincided with the top of the fuselage as in the ASW case. Sweep was increased to −30 deg, and wing root incidence was modified to increase the leading-edge height from the fuselage centerline (Figs. 13 and 14). The other components of the model were identical on all tests. The model consisted of a hardback with external body pieces. A set of canards was fabricated to provide limited assessment of canard effects. The configuration incorporated a centerline vertical tail.

Test Results

Transonic Maneuver Condition

The wing location criteria used for the first wind tunnel entry resulted in the fabrication of the forward swept wing such that the wing root leading edge height was only 0.1875 in. above the fuselage reference line. The aft swept wing root leading-edge height was 1.0625 in. (Fig. 14). A comparison of chordwise pressure distributions at two spanwise stations farthest from the wing-body junction (ETA = 0.625 and 0.85) shows that the FSW lower surface pressure is higher than the ASW (Fig. 15). This is one mechanism that allows a forward swept wing to have a lower profile drag, provided that the condition of equal shock sweeps are satisfied throughout the full wing span (Fig. 4). Although this desired pressure trend exists in some regions of the FSW during the first test, a comparison of drag at the maneuver condition shows that the FSW drag is considerably higher than the ASW for a wing-body configuration (Fig. 16). An examination of the first set of pressure and oil flow data shows that loss of lift (Fig. 17) and separation (Fig. 18) is occurring in the vicinity of the wing-body junction. The effects of the addition of canards are to improve the FSW drag (Fig. 19), (e.g., $\Delta C_D = 200$ counts for a −5-deg deflection at $C_L = 0.9$) and provide a marked straightening of the oil flow patterns on the inboard areas affected by canard downwash (Fig. 20). The same canards provided no appreciable effects on the ASW (Fig. 21). These findings indicate that the FSW was mislocated so that the inboard wing area was operating in a region of excessive fuselage upwash, thereby causing premature separation and shock unsweeping. This made the first FSW vs ASW comparisons unsatisfactory since the condition of near identical flow (i.e., equal shock sweeps and spanloads) was not satisfied.

In an unpublished study conducted by the External Aerodynamics Group, using a modified transonic small disturbance code on the FSW, it was found that improvements in chordwise pressure (Fig. 22) and spanwise load distribution can be obtained by varying the wing height from $WL = 0.2$ to 0.8. The shock shows a rearward movement (Fig. 23), and the spanload increases near the fuselage centerline (Fig. 24). Guided by these calculations, the FSW was modified in order to make the crest point of the centerline

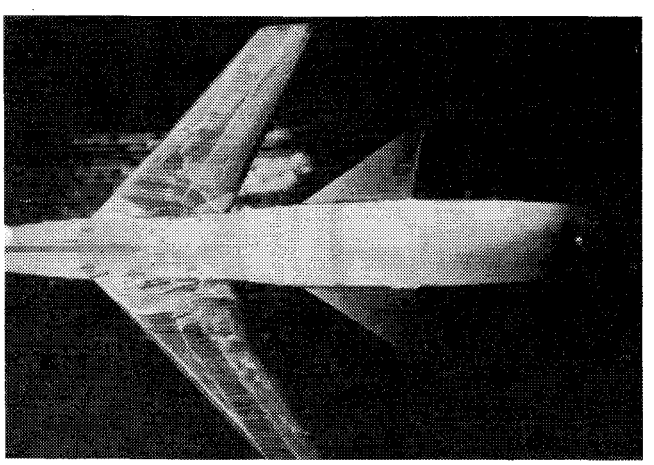

Fig. 20 Canard effects (FSW).

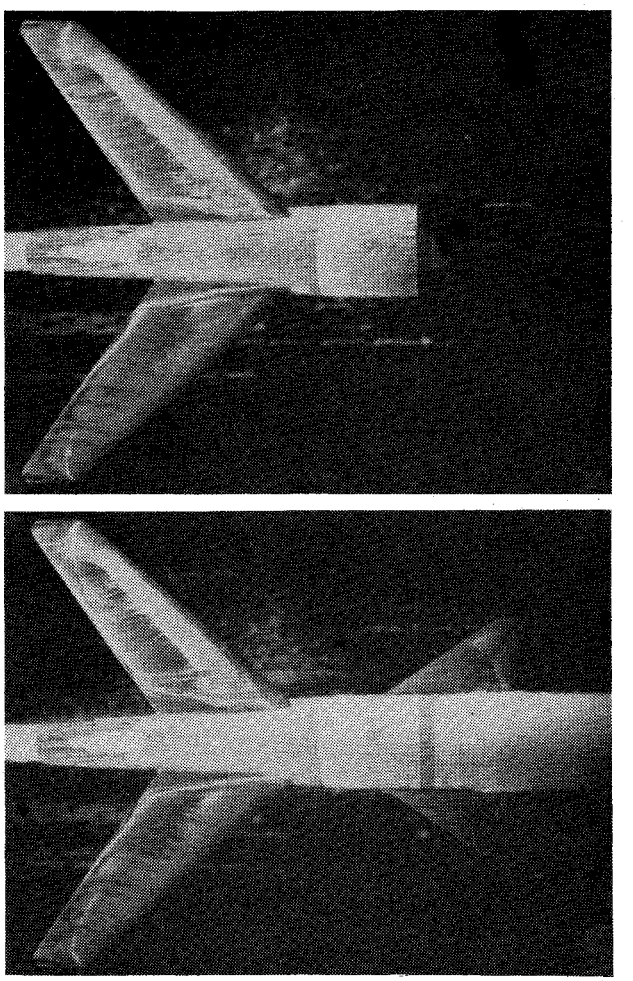

Fig. 21 Canard effects (ASW).

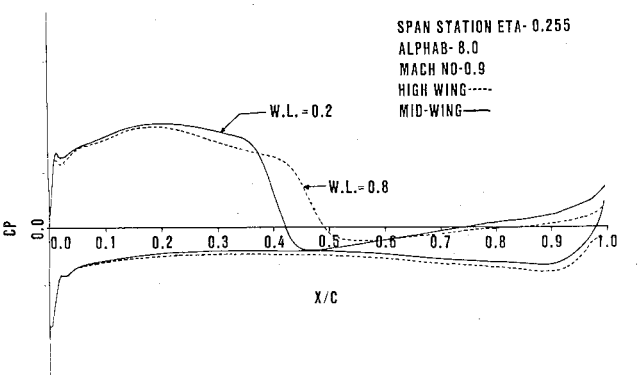

Fig. 22 Effect of wing height on chordwise pressure distribution.

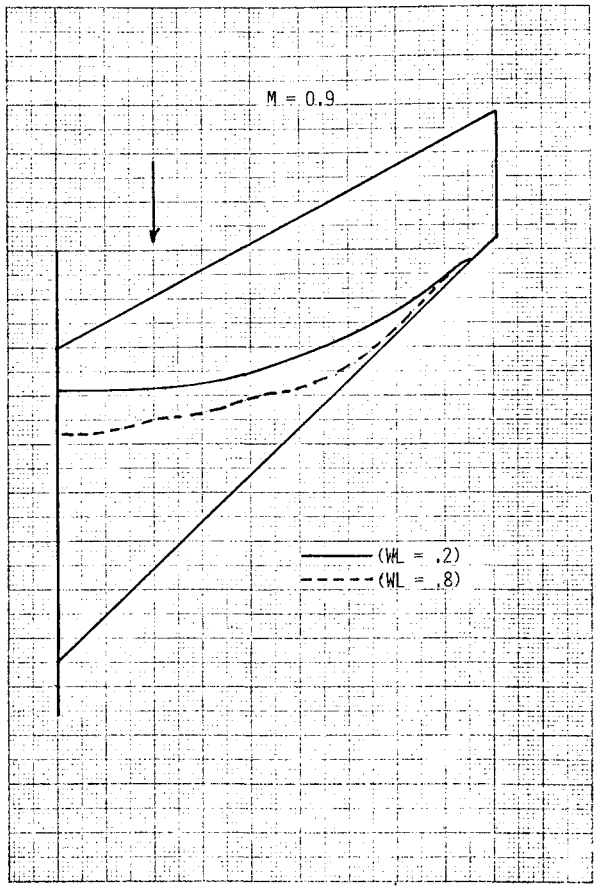

Fig. 23 Effect of wing height on shock location.

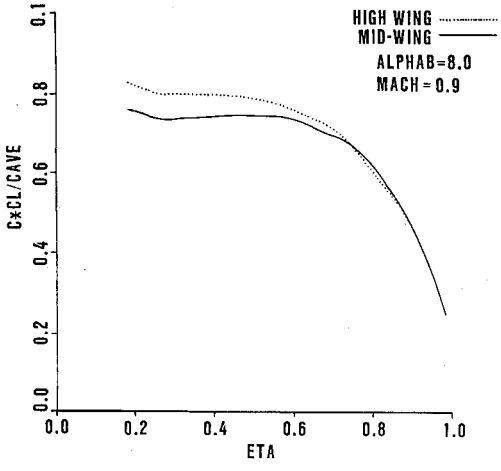

Fig. 24 Effect of wing height on spanwise load distribution.

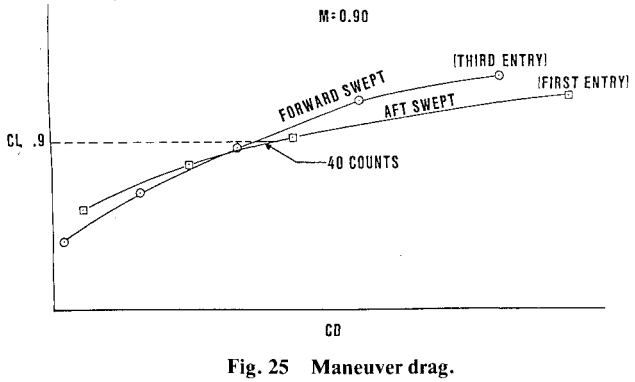

Fig. 25 Maneuver drag.

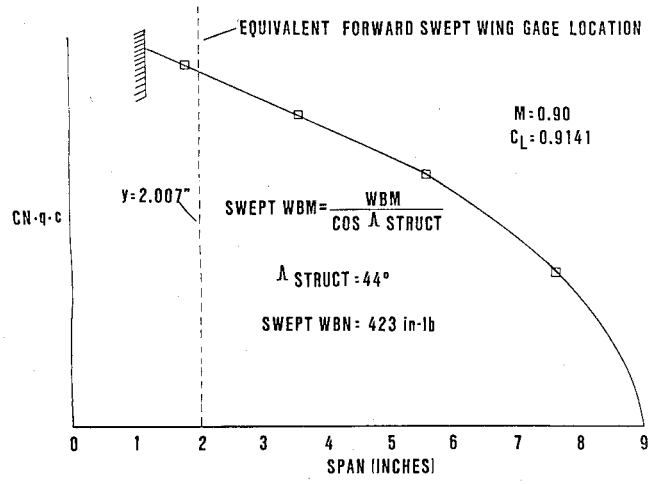

Fig. 26 Aft swept wing bending moment.

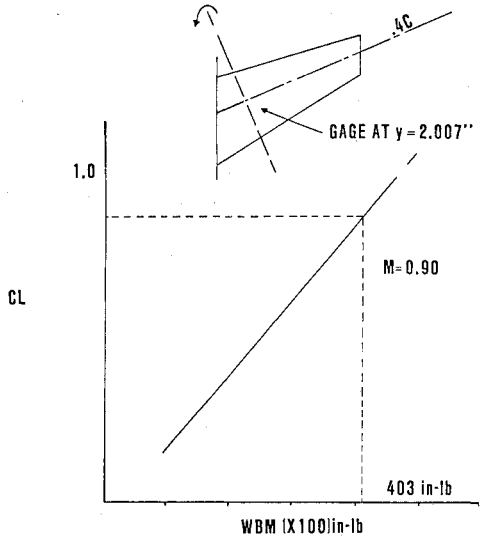

Fig. 27 Forward swept wing bending moment.

airfoil coincident with the top of the fuselage. This modification raised the root leading edge to 0.625 in. above the fuselage reference line. Matching the ASW and FSW root leading-edge heights was desired, but the geometric constraint imposed by the FSW fuselage diameter and the opposite root incidence limited this wing relocation. Figure 25 shows a comparison of the modified FSW (third entry) drag to the first entry ASW at the maneuver design condition. The FSW exhibits 40 counts lower drag than the ASW and a 235 count improvement from the first FSW entry.

Since the aspect ratios of both wings were constrained, only the maneuver profile drag reduction was directly verified. However, an indication of the potential induced drag advantage can be seen by comparing pivot bending moment data. A comparison of the ASW integrated moment of area of the spanload (Fig. 26) about an axis at $y = 2.007$ in., where the equivalent FSW bending gage is located to the direct FSW gage readings (Fig. 27), showed that the FSW bending moment was 20 in.-lb less than the ASW moment. An integrated FSW spanload was not used since no pressure data was obtained from the third wind tunnel entry.

Supersonic Cruise

A drag penalty was recorded for the FSW cruise wing at a high supersonic Mach number (2.0). For this test, only the wing camber and twist were modified. Sweeps were retained from the maneuver wing designs; consequently, the FSW

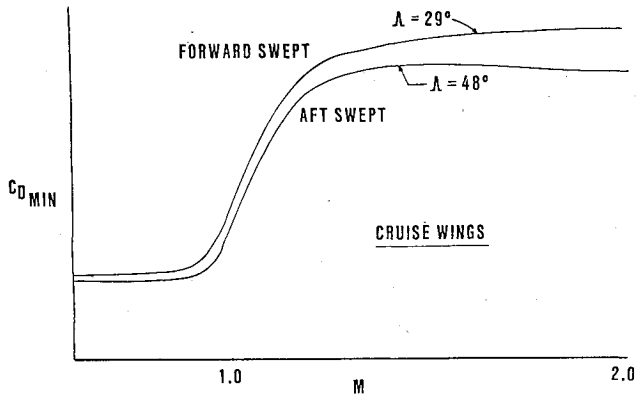

Fig. 28 Cruise wing drag.

leading edge becomes supersonic at a lower Mach number than the ASW. The same geometric reason that provides an advantage for FSW transonically may become a disadvantage at supersonic Mach numbers if the wing sweep is fixed. A better comparison for a high Mach number condition can be made by using the condition of equal leading-edge sweeps. Figure 28 shows that at lower supersonic Mach numbers, the difference in drag is less than at the higher Mach numbers.

Concluding Remarks

Some of the results of a wind tunnel investigation of the aerodynamic characteristics of forward swept wings have been discussed. It was shown that under identical transonic maneuver design conditions, a forward swept wing can be designed to provide lesser drag than an equivalent aft swept wing. A potential for further drag reduction was demonstrated by comparing the wing bending moments and showing that the FSW bending moment is lower, thereby allowing a possible growth in FSW aspect ratio and reduced induced drag. The achievement of comparable point design transonic maneuvering drag indicates that current aft swept wing aerodynamic design methods can be used to design forward swept wings with little or no modifications. Additionally, FSW drag and wing inboard pressures exhibit extreme sensitivity to wing root height and incidence variations as a result of a strong and synergistic effect of the fuselage and wing upwash on the inboard wing flow. This area requires careful consideration during the wing design process.

References

[1] Uhuad, G.C., Weeks, T.M., and Large, R., "An Experimental Investigation of the Aerodynamic Characteristics of Forward Swept Wings," Paper 21 presented at the AGARD Symposium on Subsonic/Transonic Configuration Aerodynamics, Munich, Germany, May 1980.

[2] Krone, N.J. Jr., "Divergence Elimination with Advanced Composites," AIAA Paper 75-1099, Aug. 1975.

[3] "Propulsion Wind Tunnel Facility," Vol. 4, in *Test Facilities Handbook,* 10th ed., Arnold Engineering Development Center, May 1975.